Isomerization of Asp–Asp Motif in Model Peptides and a Monoclonal Antibody Fab Fragment

LI YI,[1] NIA BECKLEY,[1] BENSON GIKANGA,[1] JENNIFER ZHANG,[2] Y. JOHN WANG,[3] HUNG-WEI CHIH,[1,4] VIKAS K. SHARMA[1]

[1]Early Stage Pharmaceutical Development, Genentech, South San Francisco, California 94080

[2]Protein Analytical Chemistry, Genentech, South San Francisco, California 94080

[3]Late Stage Pharmaceutical Development, Genentech, South San Francisco, California 94080

[4]Pharma Technical Regulatory, Genentech, South San Francisco, California 94080

Received 2 August 2012; revised 16 November 2012; accepted 28 November 2012

Published online 20 December 2012 in Wiley Online Library (wileyonlinelibrary.com). DOI 10.1002/jps.23423

ABSTRACT: Isomerization of aspartyl (Asp or D) residues is a critical degradation route to consider for stable monoclonal antibody formulations. Among the known hotspot sequences, the DD motif is relatively understudied. To gain mechanistic insights, we used model hexapeptides, YADXFK, YADDXK, and DIDDDM, as surrogates for the hotspots in a Fab protein (YADDFK and DIDDDM), to characterize the rate-pH profile of Asp isomerization. Compared with the YADGFK peptide, isomerization of D3 (the first D in the DD pair) in YADDFK was highly pH dependent. Comparison of rate-pH profiles of YADDFK, YADNFK, and YADHFK revealed a charge effect of the $n + 1$ residue—isomerization rate is accelerated by the positive side chain and reduced by negative side chain at $n + 1$ residue. Studies on YADDFK, YADDAK, and YADDGK indicated a mutual impact of D3 and D4 on their respective isomerization rates through charge effect. Comparison of rate-pH profile of DIDDDM sequence in peptide models with that in the complementary determining region of the Fab showed a faster rate in the Fab than in peptides, presumably because of contribution from structural factors in the former. © 2012 Wiley Periodicals, Inc. and the American Pharmacists Association J Pharm Sci 102:947–959, 2013

Keywords: Asp–Asp motifs; isomerization; kinetics; monoclonal antibody Fab

INTRODUCTION

Isomerization of aspartyl residues (Asp or D) is a common degradation pathway that leads to product heterogeneity in monoclonal antibodies (mAbs).[1] This nonenzymatic reaction contains two major steps: (1) formation of a succinimide intermediate (Asu) resulting from the attack of the backbone amide of the $n + 1$ residue on the γ-carbonyl of Asp (molecule A to B to C, Scheme 1); and (2) hydrolysis of Asu into either an Asp or an isoaspartyl (IsoD) residue (molecule C to D to E, Scheme 1).[2–5] The degraded protein containing Asu and IsoD can be measurable by chromatographic methods including ion exchange, hydrophobic interaction, or reversed phase (peptide mapping) and is reported to increase on storage.[6–8] Although the IsoD only increases the side chain by one methylene group, it can potentially change the biophysical or pharmacokinetic property of a mAb and affect the potency by disturbing specific antigen binding, depending on the modification site on the molecule.[9] With these potential pharmaceutical and biological impacts, Asp isomerization, especially when occurring at the complementarity-determining region (CDR) of a mAb, is usually considered to be a critical quality attribute.

Asp isomerization has been studied for decades. Among others, two factors that have the greatest impact on isomerization rate are the pH and the sequence dependence (identity of the $n + 1$ residue). In the pH range commonly used to formulate therapeutic proteins (pH 4–7), the isomerization rate usually follows a decreasing trend as pH increases.[10] The $n + 1$ residue affects the isomerization rate primarily by sterically hindering the attacking nitrogen with its side chain; therefore, bulkier side chains result

Correspondence to: Li Yi (Telephone: +650-225-1108; Fax: +650-225-3613; E-mail: yi.li@gene.com)

Journal of Pharmaceutical Sciences, Vol. 102, 947–959 (2013)

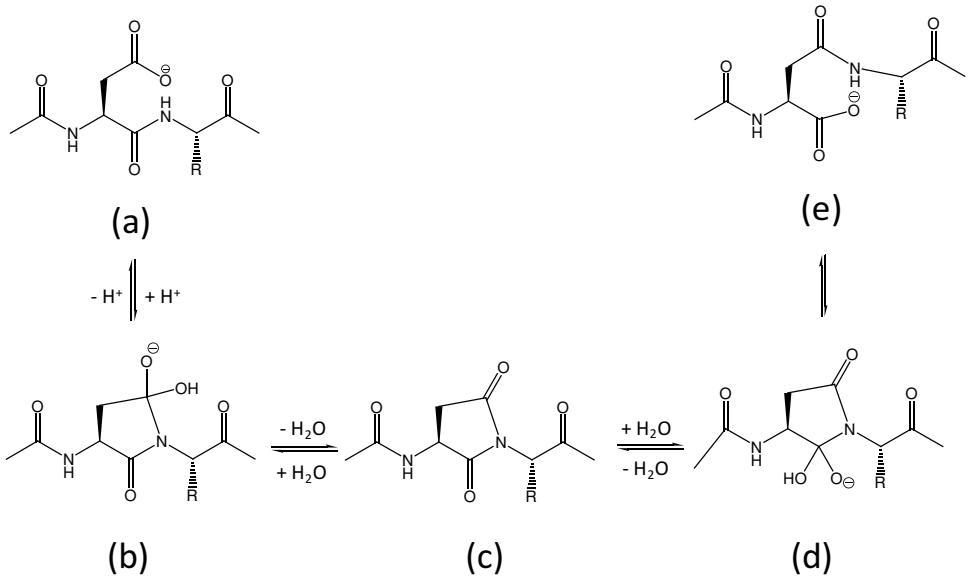

Scheme 1. Mechanism of Asp isomerization. (a) Asp, (b) tetrahedral intermediate formed on side chain, (c) succinimide intermediate (Asu), (d) tetrahedral intermediate formed on backbone, (e) Iso–Asp (IsoD).

in slower isomerization.[11] The "hotspot" sequences that are commonly identified in protein and peptide studies include DG,[7,8,11–16] DS,[2,11,16] DT,[17] DA,[16] and DH.[18,19] Other factors including protein three-dimensional structure[7,15,20] and dielectric constant of solvent[21] may also alter isomerization rates and require further mechanistic understanding. A thorough understanding of all of these factors paves the way to a more accurate prediction of the stability of hotspots, which will facilitate the selection of therapeutic candidates with good chemical stability for pharmaceutical development before any costly investments are made.

One hotspot sequence studied in recent years is the Asp–Asp motif. Xiao and Bondarenko[22] reported isomerization in an Asp-rich sequence in CDR of an Immunoglobulin G2 (IgG2). This hotspot motif was not fully characterized nor compared with the other well-known hotspots. Therefore, we were motivated to further characterize isomerization of this motif and ultimately gain better mechanistic insights. To this end, we investigated a Fab containing two DD motifs, one on the light-chain CDR1 and the other on the heavy-chain CDR2. Isomerization sites in this Fab were identified by Zhang et al.[23] using ^{18}O labeling and mass spectrometry (MS). We first obtained the isomerization rates of the DD motif at various pH values in our study using model hexapeptides that share the same sequences as present in the Fab CDRs, that is, DIDDDM (light-chain CDR1) and YADDFK (heavy-chain CDR2), as surrogates. Then we used YADXFK as a template, where X is D, H, or N, to study the effect (specifically, the charge effect) of the $n + 1$ residue on the isomerization rate. The mutual impact of the two Ds in the DD motif was also investigated using YADDXK variants. Finally, isomerization rates on model peptides and the Fab protein were compared to probe the effect of protein structure.

MATERIALS AND METHODS

Materials

Hexapeptides, YADXFK (X = G, D, N, H) and YADDXK (X = G, D) were synthesized at Genentech, Inc. (South San Francisco, California) using standard solid-phase Fmoc chemistry. The N termini were capped with acetyl groups and the C termini were capped with amides. The recombinant humanized mAb fragment, the Fab, was manufactured at Genentech, Inc. The chemicals used for making the buffer were purchased from Sigma–Aldrich (St. Louis, Missouri) or Fisher Scientific (Pittsburgh, Pennsylvania). Endoproteinase Lys-C was obtained from Sigma–Aldrich.

Peptide Isomerization

Peptides at a final concentration of 0.2 mM were prepared in different buffers (20 mM buffer concentration) and 150 mM NaCl and incubated at 37°C for kinetic study. The buffers were sodium acetate (NaAc) at pH 3.6, 4.5, 5.0, and 5.5; histidine chloride (HisCl) at pH 5.5, 6.0, and 6.5; sodium phosphate (NaPi) at pH 6.5, 7.0, and 8.0; and Tris at pH 8.0 and 9.0. The actual pH was measured at room temperature and was corrected to values at 37°C by corresponding temperature-dependent factors (acetate −0.0002 pH unit/°C, histidine −0.015 pH unit/°C, phosphate

−0.0028 pH unit/°C, and Tris −0.028 pH unit/°C).[24,25] Samples were prepared in a 96-well plate format on a Biomek® FX^P station (Beckman Coulter, Indianapolis, Indiana). The plates were sealed on PlateLoc sealer (Agilent Technologies, Santa Clara, California) and bagged into Mylar bags (GE Healthcare Biosciences, Pittsburgh, Pensylvania) to avoid water evaporation. Time courses were obtained for each peptide at each individual condition.

Reversed-Phase High-Performance Liquid Chromatography

Peptide samples were analyzed by reversed-phase high-performance liquid chromatography (RP-HPLC) using a Jupiter C18 column (Phenomenex, Torrance, California; Cat No. 00F-4053-B0) on an Agilent 1200 HPLC system (Agilent Technologies, Santa Clara, California). Column temperature was set to 35°C. Samples were eluted at 0.25 mL/min with buffer A [0.1% trifluoroacetic acid (TFA) in water] and buffer B (0.1% TFA in acetonitrile). Degradation peaks of YADDFK, YADGFK, YADHFK, and YADNFK peptides were resolved with a gradient of 0%–36% buffer B over 20 min, whereas YADDAK and YADDGK were resolved with a gradient of 0%–12% buffer B over 20 min. The UV absorbance at 280 nm was followed and relative peak area was used to quantify each of the degradants.

Peak Assignment

For peak assignment, the RP-HPLC was directly coupled to a LTQ Orbitrap mass spectrometer (Thermo Fisher Scientific, Bremen, Germany) equipped with an electrospray ionization source. The spray voltage was 4.5 kV, and the capillary temperature was 300°C. The mass spectrometer was operated in the data-dependent mode to automatically switch between MS and tandem mass spectrometry (MS–MS). Survey full-scan MS spectra were acquired from *m/z* 300 to 2000 in the FT-Orbitrap with a resolution of R = 60,000 at *m/z* 400. The five most-intense ions were fragmented in the linear ion trap using collisionally induced dissociation at a normalized collisional energy of 35%. On the RP-HPLC profiles, the *m/z* −18 peaks were assigned as Asu, and the MS–MS data were used to determine the position of Asu when multiple Asp residues were present. Because IsoD and Asp were nondistinguishable by *m/z*, hexapeptides with L- or D-IsoD incorporated into either DD site were synthesized and coinjected with stressed native peptides to locate the corresponding IsoD species on the native RP-HPLC profile.

Protein Isomerization

The Fab protein was dialyzed into three 20 mM buffers (pH 4.5 NaAc, pH 5.5 HisHCl, and pH 7 NaPi) with 150 mM NaCl and the final concentration adjusted to 10 mg/mL. Samples were aliquoted into 2-cm^3 serum vials, stoppered and capped, and then incubated at 37°C for up to 2 months.

Peptide Mapping

Protein samples (100 μL) at 10 mg/mL were pretreated with 900 μL of sulfitolysis reagent [6 M guanidine hydrochloride, 360 mM Tris, 2 mM ethylenediaminetetraacetic acid (EDTA), 127 mM sodium sulfite, 26 mM sodium tetrathionate (pH 8.6)] at 37°C for 20 min. The samples were then buffer exchanged on PD-10 columns (GE Healthcare, Cat No. 17-0851-01) into digestion buffer [25 mM Tris, 1 mM EDTA (pH 8.3)]. The protein collected was then mixed with Lys-C enzyme at a ratio of 55:1 and followed by incubation at 37°C for 5 h. The digestion was then quenched by adding 15 μL of 10% TFA. The samples were loaded on a Zorbax 300SB-C8 column (Agilent, Cat No. 863973-90) and eluted at 1 mL/min over 92 min using a gradient of buffer A to 90% of buffer B.

RESULTS AND DISCUSSION

The DD motif is a relatively understudied isomerization hotspot and is important to consider when formulating therapeutic mAbs or Fabs. In this study, we examined the isomerization of the DD motif using model peptides. Such peptides that carry the CDR sequence of mAbs or Fabs are good experimental surrogates as they can be stressed in wider pH ranges and analyzed in higher throughput. Isomerization of DD presents an interesting case because besides size, the charge on the $n + 1$ residue side chain may also impact the rate-pH profile. Furthermore, because both Ds in a DD motif have the potential to isomerize, the mutual impact of two Ds may be reflected on their rate-pH profile as well. Last but not least, it is useful and practical to understand how the model peptides represent protein in terms of isomerization rate and whether protein structure changes the isomerization rate of the same sequence. To gain understanding on these questions, we present below the characterization and comparison of rate-pH profiles of the DD containing model peptides, model peptide variants, and the Fab protein.

Peptide Degradation and Kinetics Modeling

Characterization of Degradation Products

In general, the Asp-containing model peptides degraded to IsoD and Asu species after being incubated at 37°C. The degradation products were separated and quantitated using RP-HPLC. The total integrated peak area of all the samples after 63-day incubation at 37°C, compared with that at time zero, was 97%–102%. Although the plates were well sealed and fully covered, the final volume of the

samples, considering slight evaporation of water, was above 90%. With that, the mass balance should be above 90%. Consistent in all tested peptides, the IsoD species eluted earlier than Asp, whereas the Asu species eluted after the Asp. The Asu species was undetectable at higher pH because of fast hydrolysis. Specifically, for YADGFK and YADHFK with a single Asp residue, isomerization was the major degradation pathway accompanied by mild enantiomerization. Enantiomerization of Asp is believed to occur through Asu, because the α proton becomes more acidic when the ring structure is formed.[4,5,26–28] The L- and D-forms of Asu can then hydrolyze to either L- and D- forms of IsoD, respectively, and/or L- and D- forms of Asp, respectively, through the same mechanism and therefore are assumed to have similar isomerization rate constants. For the DG peptide, the D-IsoD showed as a small resolved peak next to the L-IsoD with a later retention time, whereas the D-Asu showed with a slightly earlier retention time as the L-IsoD. For other peptides, the D-species eluted as a shoulder peak to the L-species or even coeluted in some cases. In all cases, the L-species are dominating (as expected, because the starting species is L-form) and D-species did not build to significant amounts. The rate of Asu enantiomerization was not a point of concern in this study; therefore, the L- and D- species were combined for analysis.

Backbone hydrolysis products were also observed, but only at pH 3.6 and 4.5. These cleavage products were confirmed with MS analysis and eluted far early in the RP-HPLC profile. After 63 days of incubation at 37°C, less than 5% of the cleavage products were observed for all the peptides. Given the low abundance of the cleavage products, these peaks were excluded from the total integration and should pose minimum impact on kinetic-fitting accuracy. For peptides with double Asp residues, YADDFK (Fig. 1a), YADDAK, and YADDGK, isomerization was observed on both Asp residues. The degradation products of these peptides contained a mix of IsoD, Asu, and Asp on both sites. The Asu–Asu was eluted the last on the RP-HPLC because of presumably higher hydrophobicity. It was observed only at pH <5 when the hydroxide-catalyzed Asu hydrolysis is relatively slow. The isoD–isoD species, which should elute the earliest among the isomerization degradants, were not observed for the DD peptides. It may coelute with some cleavage products, but the total front peak percentage is <5%. This species could also present under the detectable limit because Asu hydrolysis is slow at acidic pH and the overall isomerization rate reduces at basic pH. In any case described above, taking the isoD–isoD off the reaction scheme should not have a considerable impact on the rate determination. For the YADNFK peptide (Fig. 1b), deamidation of asparagine occurred above pH 6.5 in addition to isomerization of Asp. All peaks were assigned with confidence using multiple analytical methods as described in section *Materials and Methods* (data not shown). Degradation products of the YADXFK and YADDXK peptides at various pH values were quantified and plotted against time (example shown in Figs. 2 and 3). These time courses were used for kinetic fitting to obtain k_{obs}.

The degradation profile of DIDDDM was complicated by isomerization on every Asp residue in this peptide. The chromatogram of the degraded sample contains too many peaks (>15 degradation peaks, data not shown) to accurately assign their identity. Therefore, the decay of the main peak was analyzed instead of resolving every single degraded species.

Kinetic Modeling of Peptide Isomerization

Two assumptions were applied to kinetic models based on the observed data: (1) enantiomerization products were combined as one species in the analysis; (2) cleavage products were excluded from the data because they presented at low abundance (<5%) across the time course. Considering only Asp, Asu, and IsoD species, the simplest kinetic model to describe Asp isomerization was to fit a single exponential decay on the main peak by assuming an irreversible first-order mechanism.[15] This model was widely used to quickly rank order isomerization rates, but at the cost of losing data-fitting accuracy and mechanistic details. A more comprehensive model can be used[10] (Scheme 2, Model 1′) to derive stepwise rate constants for Asu formation and hydrolysis. However, in this study, the Asu species were onlydetectable at pH <5. To use a consistent model throughout the tested pH, a modification was made by pooling the corresponding Asu and IsoD as total degradants (Scheme 2, Model 1–3). As an example, data fitting of the YADGFK time course at pH 3.6 using Models 1′ and 1 resulted in close k_{obs} values (0.067 vs. 0.069 day^{-1}; Fig. 2), thereby confirming that Model 1 can substitute for Model 1′ even when Asu is observable.

Model 1 in Scheme 2 depicts a simple equilibrium between an Asp residue and its degradants. This model was applied to the single-Asp-containing peptides, YADGFK and YADHFK, as well as to the DIDDDM peptide (assuming that the main peak degrades to a pool of products). The concentration of each species as a function of time is shown in Eqs. 1 and 2, where A_0 is the initial concentration of the Asp peptide. In this case, the k_{obs} is the sum of the forward rate constant (k_f) and the reverse rate constant (k_r).

$$[\mathrm{Asp}]_t = \frac{k_r A_0}{k_r + k_f} + \frac{k_f A_0}{k_r + k_f} e^{-(k_r + k_f)t} \quad (1)$$

$$[\mathrm{Asu} + \mathrm{IsoD}]_t = A_0 - A_t \quad (2)$$

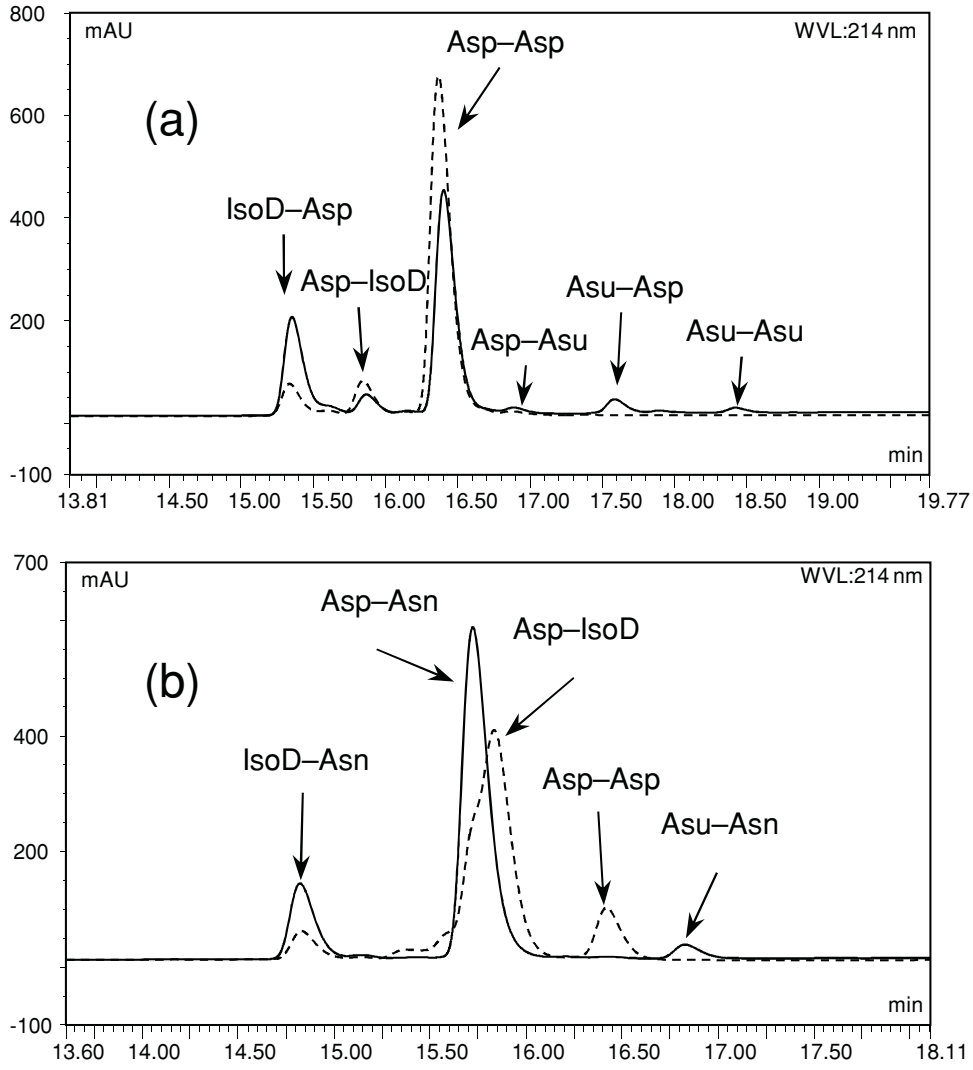

Figure 1. RP-HPLC chromatogram of the (a) YADDFK and (b) YADNFK peptides stressed at 37°C for 63 days in pH 5.0 sodium acetate (solid line) and sodium phosphate pH 8.0 (dashed line).

Both dependent variables, Asp decay and degradants' growth, were fit globally to the equation set using Scientist software (Micromath Research, St. Louis, Missouri) to obtain both the forward and reverse rate constants. The ratio k_f:k_r represents the final equilibrium ratio of IsoD to Asp. Between pH 5 and 7, this number falls in the range of 2.3–2.7, which is slightly lower than the reported 3–4 for the VYPDGA peptide.[10] These data indicate that the neighboring groups may interfere with the thermodynamic equilibrium between the isoD and Asp.

In Model 2 in Scheme 2, the isomerization of double Asp peptides (YADDFK, YADDAK, and YADDGK) was described as two independent reactions on each Asp residue. Irreversibility was assumed because isomerization at multiple Asp sites was involved. For degradation at each Asp, the corresponding Asu and IsoD were combined as the degradation product. For these peptides at pH 3.6 and 4.5, the Asu–Asu was also observed as a degradant; therefore, added to the total products for each pathway. Because Asu–Asu as a single species was included in both degradation pathways, the decay of starting peptide was not used to fit the parameters (i.e., Eq. 3 was excluded, Eqs. 4 and 5 were used) for reactions at pH 3.6 and 4.5. Experimental data were fit to Eqs. 3–5, where α is the ratio of the rate constants of the two reactions. The rate constant is therefore αk for D3 and $(1-\alpha)k$ for D4. As an example, fitting results of YADDFK are shown in Figure 3.

$$[\text{Asp.Asp}]_t = A_0 e^{-kt} \tag{3}$$

$$[\text{IsoD.Asp} + \text{Asu.Asp}]_t = \alpha A_0 (1 - e^{-kt}) \tag{4}$$

$$[\text{Asp.IsoD} + \text{Asp.Asu}]_t = (1-\alpha) A_0 (1 - e^{-kt}) \tag{5}$$

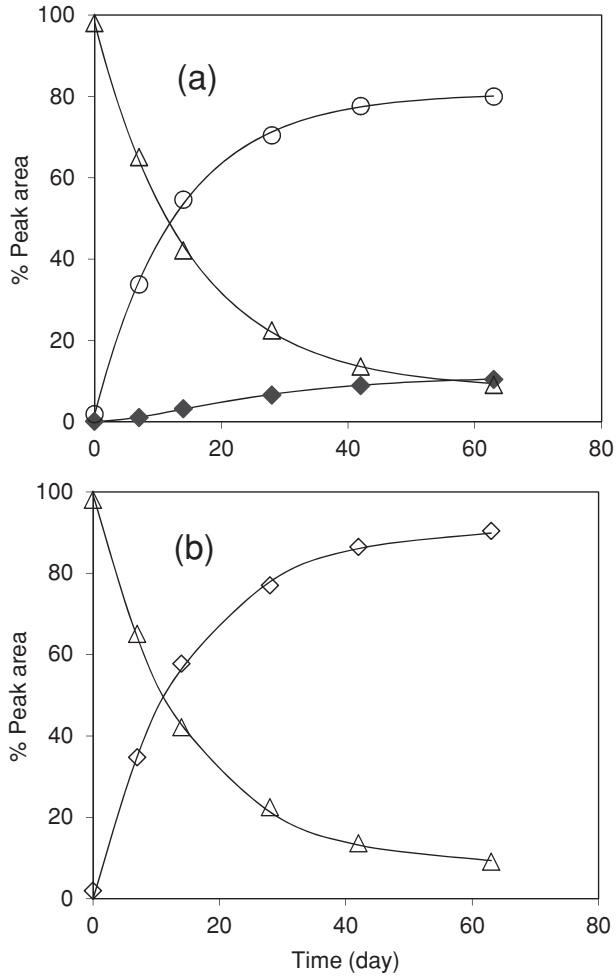

Figure 2. Time course of YADGFK peptide at pH 3.6 fitted by (a) Model 1′ and (b) Model 1. Model fittings are shown as solid lines. Experimental data are shown for Asp (open triangle), IsoD (closed diamond), Asu (open circle), and sum of IsoD and Asu (open diamond). All experimental data are the average of duplicates.

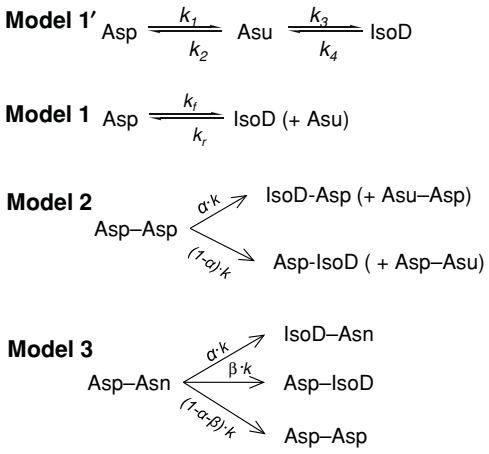

Scheme 2. Kinetic models for YADXFK and YADDXK peptides isomerization.

The YADNFK peptide followed Model 1 in Scheme 2, when pH was below 6 because no deamidation was observed. However above pH 6, the deamidation on N4 led to the formation of Asp and IsoD at this position. Model 3 was constructed to describe this situation, and Eqs. 6–9 were derived, where α, β, and $(1-\alpha-\beta)$ are fractional factors of each branching reaction. One analytical challenge with this peptide was that the main peak, Asp–Asn, and one of the deamidation products, Asp–IsoD, were coeluted on RP-HPLC (Fig. 1b). This challenge was addressed by assuming that the ratio of Asp–IsoD to Asp–Asp equaled that of IsoD to Asp in the YADGFK peptide at each pH. With the amount of Asp–Asp obtained from the RP-HPLC profile, the Asp-IsoD can be calculated based on the ratio described. With the Asp–IsoD peak area subtracted from the coeluted peak, the area of the main peak, Asp–Asn, can be obtained.

$$[\text{Asp.Asn}]_t = A_0 e^{-kt} \tag{6}$$

$$[\text{IsoD.Asn}]_t = \alpha A_0 (1 - e^{-kt}) \tag{7}$$

$$[\text{Asp.IsoD}]_t = \beta A_0 (1 - e^{-kt}) \tag{8}$$

$$[\text{Asp.Asp}]_t = (1 - \alpha - \beta) A_0 (1 - e^{-kt}) \tag{9}$$

Using the above-described models for respective peptides, the rate constants of the isomerization reactions on each Asp residue were determined from the kinetic fitting (Table 1) and used to generate rate-pH profile (Figs. 4,5,6 and 8). The rate constants of Asp-containing peptides reported in literature are in close agreement with the values obtained in this study. For example, the rates of VYPDGA reported by Oliyai and Borchardt[10] are 0.067 day^{-1} at pH 4, 0.031 day^{-1} at pH 5, and 0.0175 at pH 7.4; that of VYPDAA and VYPDHA reported by Radkiewicz et al.[15] are both 0.0026 at pH 7.4; and that of a DA peptide reported by Sadakane et al.[29] is 0.0011 at pH 7.4.

Rate-pH Profile of DG Versus DD

The rate-pH profiles of peptides were obtained by plotting k_{obs} against pH. The measured pH was corrected by the temperature-dependence factor of each buffer to render pH values at the tested temperature, 37°C. Four biological buffer series commonly used for mAb formulation were selected to cover a pH range of 3.6–9 (Table 1). The calculated ionic strength for all the buffers with 150 mM NaCl is 152–203 mM. No impact of ionic strength on isomerization rate was observed in this range because similar rates were observed for different buffer species at similar pH but with different ionic strength; for example, pH 6.28 HisHCl at 153 mM ionic strength versus pH 6.13 NaPi at

 DOI 10.1002/jps

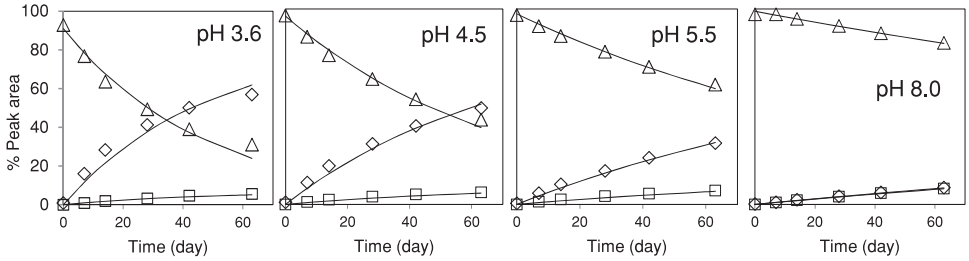

Figure 3. Time course of YADDFK at selected pH values fitted by Model 2. Model fitting are shown as solid lines. Experimental data are shown for Asp–Asp (open triangle), combined IsoD–Asp and Asu–Asp (open diamond), combined Asp–IsoD, and Asp–Asu (open square). All experimental data are the average of duplicates. The pH values selected are pH 3.6 and 4.5 with sodium acetate, pH 5.5 with histidine chloride, and pH 8.0 with sodium phosphate.

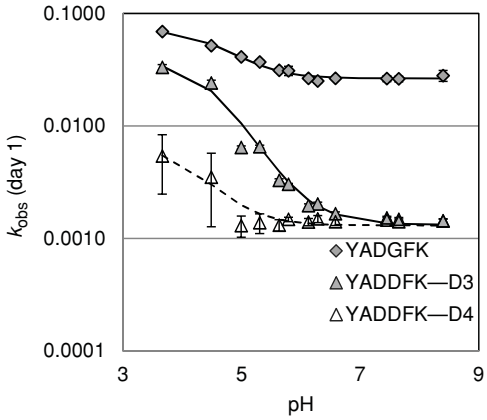

Figure 4. Rate-pH profile of the peptide YADGFK and YADDFK.

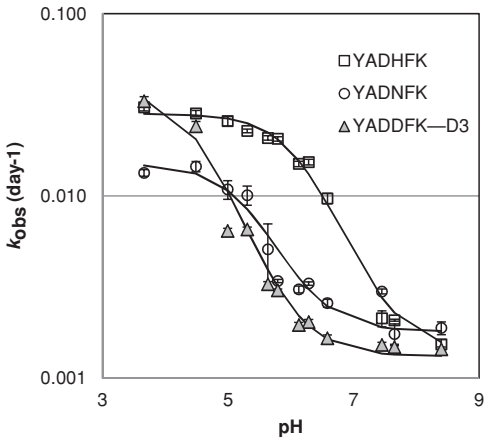

Figure 5. Rate-pH profile of D3 in YADDFK, YADHFK, and YADNFK peptides.

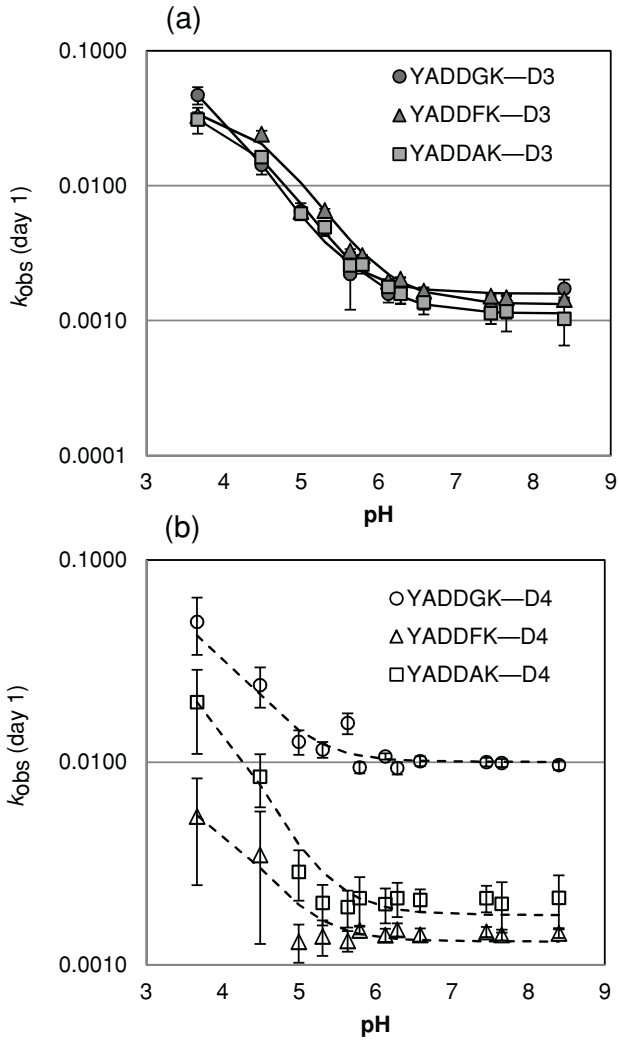

Figure 6. Rate-pH profile of (a) D3 and (b) D4 in YADDFK, YADDAK, and YADDGK peptides.

170 mM ionic strength, and pH 7.65 NaPi at 203 mM ionic strength versus pH 7.45 Tris at 166 mM ionic strength. Different buffer species were tested at overlapping pH values (e.g., NaAc and HisHCl at pH 5.5) to also examine the buffer catalysis effect. The results showed that the isomerization rate was not buffer-species dependent because no systematic increase or decrease in k_{obs} was observed in any buffer (Figs. 4–6 and 8). This result agreed with a previous report by Oliyai and Borchardt,[10] who demonstrated no difference in a DG-peptide isomerization rate when incubated in various buffers at 5–100 mM. Buffer catalysis of isomerization was observed by Capasso et al.[30] for

Table 1. Rate Constants (k_{obs}) of All Peptides in 10^{-3} day^{-1}

	pH	YADGFK D3	YADHFK D3	YADNFK D3	YADDFK D3	YADDAK D4	YADDGK D3	DIDDDM D4	D3	D4	All[a]
NaAc	3.66	69.0 ± 1.3	30.6 ± 1.3	13.4 ± 0.6	33.1 ± 1.9	5.4 ± 2.9	30.9 ± 6.8	19.8 ± 8.8	46.9 ± 6.9	49.5 ± 15.6	72.1 ± 2.0
	4.49	51.5 ± 1.4	28.3 ± 1.1	14.5 ± 0.9	24.1 ± 1.5	3.5 ± 2.2	16.2 ± 1.5	8.5 ± 2.5	14.2 ± 2.2	24.0 ± 5.4	52.7 ± 2.0
	4.99	41.1 ± 1.4	25.7 ± 1.5	10.8 ± 1.3	6.4 ± 0.2	1.3 ± 0.3	6.2 ± 0.5	2.9 ± 0.8	6.5 ± 0.9	12.6 ± 1.7	33.5 ± 0.7
	5.63	31.2 ± 1.1	20.8 ± 0.6	5.1 ± 1.9	3.3 ± 0.1	1.3 ± 0.2	2.6 ± 0.3	1.9 ± 0.4	2.2 ± 1.0	15.6 ± 1.8	17.1 ± 1.0
HisHCl	5.30	37.0 ± 1.5	22.7 ± 0.5	10.1 ± 1.2	6.5 ± 0.2	1.4 ± 0.3	4.9 ± 0.3	2.0 ± 0.5	4.8 ± 0.6	11.6 ± 1.0	29.9 ± 1.2
	5.79	31.0 ± 2.9	20.5 ± 0.6	3.4 ± 0.1	3.0 ± 0.1	1.5 ± 0.1	2.6 ± 0.4	2.1 ± 0.6	2.7 ± 0.3	9.4 ± 0.6	13.8 ± 0.3
	6.28	25.1 ± 1.2	15.3 ± 0.5	3.3 ± 0.1	2.0 ± 0.1	1.5 ± 0.1	1.6 ± 0.3	2.1 ± 0.4	1.7 ± 0.4	9.4 ± 0.6	7.8 ± 0.2
NaPi	6.13	26.4 ± 0.6	15.0 ± 0.5	3.1 ± 0.1	2.0 ± 0.1	1.4 ± 0.1	1.8 ± 0.2	2.0 ± 0.4	1.6 ± 0.2	10.7 ± 0.4	6.9 ± 0.2
	6.58	26.5 ± 0.6	9.7 ± 0.6	2.6 ± 0.1	1.7 ± 0.1	1.4 ± 0.1	1.4 ± 0.2	2.1 ± 0.3	1.4 ± 0.3	10.1 ± 0.6	4.2 ± 0.2
	7.65	26.2 ± 1.5	2.1 ± 0.1	1.7 ± 0.2	1.5 ± 0.1	1.4 ± 0.1	1.2 ± 0.3	2.0 ± 0.6	1.3 ± 0.3	9.9 ± 0.5	3.4 ± 0.1
Tris	7.45	26.3 ± 1.5	2.1 ± 0.2	3.0 ± 0.1	1.5 ± 0.1	1.5 ± 0.1	1.1 ± 0.2	2.1 ± 0.3	1.2 ± 0.3	10.0 ± 0.5	3.6 ± 0.1
	8.40	28.0 ± 3.1	1.5 ± 0.1	1.9 ± 0.2	1.4 ± 0.1	1.4 ± 0.1	1.0 ± 0.4	2.1 ± 0.6	1.7 ± 0.3	9.7 ± 0.5	3.3 ± 0.1

[a] Main peak decay was used to fit the data.
HisHCl, histidine chloride; NaAc, sodium acetate; NaPi, sodium phosphate.

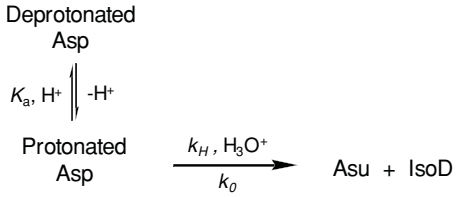

Scheme 3. The simplified pH-dependence model of Asp isomerization.

acetate buffer at above 100 mM, which was not tested in this study.

Like previously reported DG peptides,[10] YADGFK followed the same decreasing trend in rate-pH profile within pH 3.6–9 (Fig. 4, Table 1). Overall, Asu formation is the rate-limiting step in both Asp isomerization and asparaginyl deamidation.[31,32] To form Asu, the Asp side chain requires protonation to form the hydroxyl leaving group, whereas the amide on the asparaginyl side chain is readily a leaving group at pH 3.6–9. This difference in the chemistry of the leaving group resulted in opposite pH dependencies for isomerization and deamidation reactions.[1,5] In the mechanistic model described by Capasso et al.,[30] protonation of the Asp side chain was considered as a rapid equilibrium, and the rate-limiting step of the formation of Asu was the loss of the leaving group from the negatively charged tetrahedral intermediate (molecule B, Scheme 1). This step is hydronium or general acid catalyzed and therefore also favored an acidic pH. This simplified pH-dependence model is described in Scheme 3. This model assumes that only the protonated Asp side chain can undergo isomerization; and the two major pH-dependent steps are (1) protonation of Asp side chain, and (2) the hydronium-catalyzed Asu formation, whereas other pH-dependent steps like the backbone amide attack and hydrolysis of Asu are ignored because they are not rate-limiting steps. With these assumptions, the k_{obs} can be expressed as Eq. 10, where K_a is the apparent association constant of the γ-carboxylic acid on the reactive Asp, k_H is the rate constant for proton- or hydronium-catalyzed reaction, and k_0 is the rate constant for the non-acid-catalyzed reaction. This equation was also described in the work of Wakankar et al.[7] The apparent pK_a of the Asp side chain, as well as catalytic parameters, was then derived by fitting rate-pH profiles to Eq. 10 (Table 2).

$$k_{obs} = \frac{K_a}{K_a + [H^+]}(k_H[H^+]) + k_0 \quad (10)$$

The k_{obs} value for each individual Asp residue in the YADDFK peptide (surrogate for CDR sequence in Fab) was obtained from kinetic model fitting (Fig. 4, Table 1). Isomerization on D3 followed the typical

 DOI 10.1002/jps

Table 2. Asp Side Chain pK_a Values and Rate Constants for Model Peptides

	pK_a	k_H (day^{-1}M^{-1})	k_0 (day^{-1})
YADGFK—D3	4.64 ± 0.07	2031 ± 271	0.026 ± 0.001
YADHFK—D3	6.18 ± 0.08	40, 128 ± 7276	0.0014 ± 0.0009
YADNFK—D3	5.31 ± 0.13	2708 ± 749	0.0018 ± 0.0005
YADDFK—D3	4.51 ± 0.09	1206 ± 191	0.0013 ± 0.0003
YADDAK—D3	4.30 ± 0.03	740 ± 44	0.0011 ± 0.0002
YADDGK—D3	3.75 ± 0.08	463 ± 49	0.0016 ± 0.0003
YADDFK—D4	4.14 ± 0.18	76 ± 23	0.0013 ± 0.0001
YADDAK—D4	3.91 ± 0.10	232 ± 34	0.0018 ± 0.0002
YADDGK—D4	3.93 ± 0.14	519 ± 108	0.0100 ± 0.0006

decreasing trend with increasing pH, but was slower than that of YADGFK at all tested pH values. Besides, the DD peptide showed a greater pH dependence than DG, especially in the pH range of 5–7, which is the most commonly used pH range for mAb liquid formulations. In this pH range, the rate of D3 in YADDFK decreased fivefold, whereas the rate of YADGFK changed only twofold. This finding is important for formulation development because fine tuning the pH may be especially effective for DD over DG in achieving a minimal isomerization rate. Two major factors could lead to difference in D3 rate-pH profiles in DD and DG: size and charge of the $n + 1$ side chains. The kinetic parameters derived from the rate-pH profiles of DD and DG mainly differed in k_0 and k_H (Table 2). The rate constant k_0 describes non-hydronium-catalyzed formation of Asu, therefore most likely related to the bulkiness of the $n + 1$ residue. The k_H, on the contrary, describes pathways involving hydronium-assisted formation of the negatively charged tetrahedral intermediate, as well as the leaving of hydroxide to form Asu (Scheme 1), and therefore is likely affected by the charge on the $n + 1$ residue as well. Depending on the pH, the D4 side chain could display a negative charge or remain neutral. To confirm that the $n + 1$ charge affects isomerization of D3, several variant peptides were studied (see section *Effect of n + 1 Residue Charge* below).

The rate of D4 in YADDFK was, in general, suppressed by the presence of the bulky F at the $n + 1$ position and therefore showed rather insignificant pH dependence compared with D3 (Fig. 4). One interesting question to ask is whether there is any mutual impact of isomerization between the two Asp residues in a DD motif. To study this effect, peptides with faster D4 isomerization were included in this study (see section *Mutual Impact of the Two Asp Residues in DD*).

Effect of $n + 1$ Residue Charge

It is well accepted that the bulkiness of the $n + 1$ side chain impacts the isomerization rate, primarily by sterically hindering the attacking $n + 1$ amide[11] and changing backbone flexibility.[15] In addition to sequence dependence, the charge state of the $n + 1$ side chain may also play a role on isomerization rate. Bodanszky and Kwei[17] reported on the isomerization of dipeptides in an unbuffered organic solvent and found that peptides with Asp and Glu at $n + 1$ position (i.e., DD and DE) showed lower isomerization rates. A deamidation study by Li et al.,[33] on the contrary, found that the positive charge on the $n + 1$ residue accelerated the reaction. Note that the tetrahedral intermediates in deamidation and isomerization reactions share similar structures and are both negatively charged.

To confirm this effect on isomerization under formulation-relevant aqueous conditions, we obtained the rate-pH profiles on variants of YADXFK, where X = H or N. The H and N side chains are comparable with D in size, but are in different charge states in certain pH ranges. Comparison of the rate-pH profiles of these variants are shown in Figure 5. Overall, the isomerization rate of D3 follows the trend of DH > DN > DD. The apparent pK_a values of D3 derived from these rate-pH profiles are 6.2, 5.3, and 4.6 for DH, DN, and DD, respectively (Table 2). Higher apparent pK_a correlated to faster isomerization, which is consistent with the fact that more-available protonated Asp with the ready leaving group facilitates the reaction; at the same time, a positively charged $n + 1$ residue such as that in DH would also stabilize the tetrahedral intermediate. Therefore, the rate differences between DH, DN, and DD could be explained on the basis of apparent pK_a differences. The apparent pK_a of D3 could be shifted by the $n + 1$ side chain through two possible mechanisms: (1) direct interaction between the D3 and positively charged H4 could retain a proton partially on D3 at higher pH, therefore increasing the apparent pK_a; and (2) electrostatic stabilization of the deprotonated D3 by the positive charge on H4 may decrease the apparent pK_a of D3. These two theories render opposite trends of apparent pK_a shift. Because, compared with DN and DD, the apparent pK_a for DH is higher, it seems that the direct proton transfer between H4 and D3 is likely responsible for such increase. On the contrary, the apparent pK_a of D3 in DG and DD are similar, suggesting that in the case of DD a more complicated mechanism may exist in defining the rates for the DD pair. A comparison of fitted kinetic parameters indicates that k_H is a likely factor to differentiate the rates between DG and DD in the respective peptides. The k_H value is also likely to be another factor that distinguishes the rates between the DN, DD, and DH peptides (Table 2). Difference in k_H could reflect the stabilization or destabilization of the negatively charged tetrahedral intermediate by the charge on the $n + 1$ residue. Li et al.[33] reported the similar effect in peptide deamidation and argued that the electrostatic attraction or repulsion altered the rate of Asu formation.

It is interesting to note in Figure 5 that as pH decreases to 4.5 and below, the D3 in DD becomes equal or faster than that in DN. One difference between these $n + 1$ residues is that D and H have a dissociable proton on the side chain; therefore, these residues may serve as a proton source, especially at low pH, to assist D3 isomerization. The acceleration of isomerization was reported for DS and DT in organic solvent[17] and DH and DC in buffer at pH 7.4,[18] which may also be explained by the proton-donating ability of S, T, H, and C.

Mutual Impact of the Two Asp Residues in DD

The YADDAK and YADDGK peptides are expected to have faster isomerization on D4 than YADDFK because A and G have smaller side chains than F. The rate-pH profiles of D3 and D4 of these three peptides are compared in Figure 6. For D4, the rate across all pH values follows the trend of DDG > DDA > DDF (Fig. 6b), which is consistent with the bulkiness of the $n + 1$ side chain. For D3, the rate-pH profiles of all three peptides overlapped at all pH conditions, suggesting that the rate of D3 was unaffected by the rate of D4 (Fig. 6a).

Given the charge effect of the $n + 1$ residues discussed above, it is interesting to study whether the negatively charged D3 has any effect on the rate of D4 in a DD motif. It was observed that the D4 in YADDGK (Fig. 6b) isomerized slower than D3 in YADGFK (Fig. 4), especially at a higher pH. The major difference between the two DG peptides is the presence of a D at the $n - 1$ position in YADDGK, and this negatively charged residue at $n - 1$ seemed to have a similar inhibitory effect as if it was at the $n + 1$ position. The D4 in YADDGK has a lower apparent pK_a than that of D3 in YADGFK (3.93 vs. 4.64, Table 2), which also suggests that the two Asp side chains in the DD motif interact with each other. A complementary study that investigated the effect of positively charged residue at the $n - 1$ position was reported by Brennan and Clarke.[18] At pH 7.4, peptide isomerization in VYHDGA was eight times faster than in VYPDGA, suggesting an accelerating effect of H at the $n - 1$ position.

Rate-pH Profile of the Peptide Versus Protein

The isomerization of DD motifs on the Fab protein was identified by Zhang et al.[23] In their study, only one D from each site was labile (i.e., D30 in $DID_{30}DDM$ on the light-chain CDR1 and D62 in $YAD_{62}DFK$ on the heavy-chain CDR2). Here, in our study, the isomerization rates of the DD motifs on the Fab protein were obtained by following the growth of the IsoD and decay of the Asp of each reactive site using a peptide mapping method (Fig. 7). The isomerization rate of the Fab protein was determined at pH 4.5, 5.5, and 6.5 and plotted with the corresponding model peptides in Figure 8. It should be noted that the assay conditions could result in a slight underestimation of the isomerization rate in the Fab[34] as the high pH of Lys-C digestion (pH 8.3) could lead to the complete hydrolysis of the Asu intermediate to IsoD and Asp.

In general, the isomerization rate of the protein followed the same decreasing trend with increasing pH as the model peptides. The YADDFK sequence isomerized slower than the DIDDDM sequence at all tested pH values in both peptide and protein. Figure 8a shows that the isomerization rate of the D3 in YADDFK peptide is fairly comparable to that of the corresponding residue in the protein, which indicates that this region of the heavy-chain CDR2 on the Fab protein adopts a conformation with comparable flexibility as a free peptide. Many previous deamidation and isomerization studies have

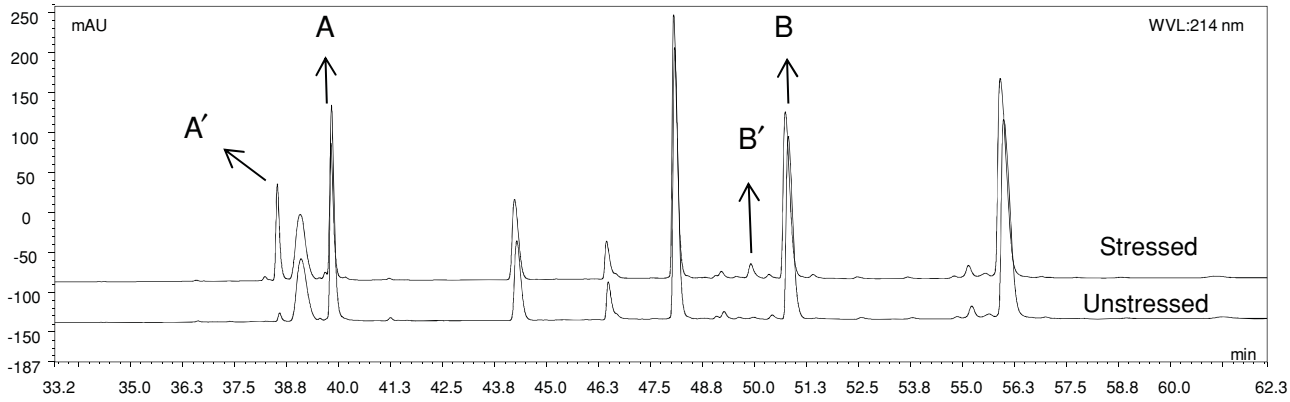

Figure 7. Lys-C peptide mapping of the Fab protein. Peak A: the light-chain peptide containing $DID_{30}DDM$ sequence; peak A′: the degraded peptide A containing $DI_{iso\text{-}}D_{30}DDM$; Peak B: the heavy-chain peptide containing $YAD_{62}DFK$; peak B′: the degraded peptide B containing $YA_{iso\text{-}}D_{62}DFK$.

 DOI 10.1002/jps

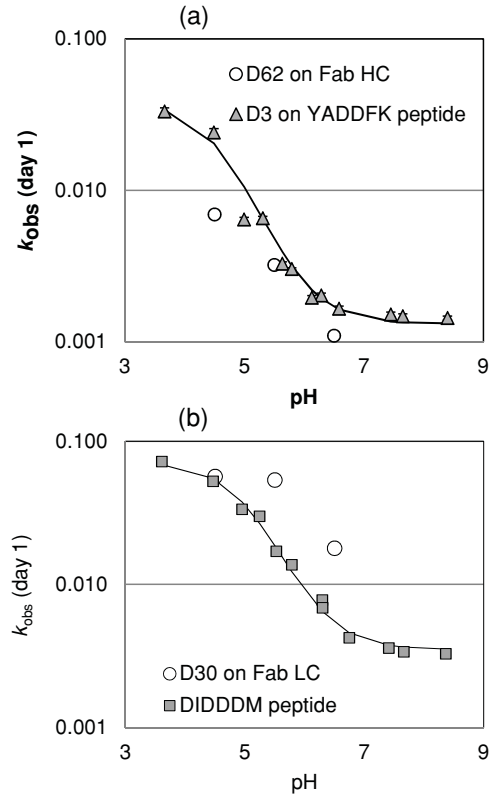

Figure 8. Rate-pH comparison of peptide (closed symbols) vs. protein (open symbols) for (a) YADDFK and (b) DIDDDM.

reported that the reactive sites residing in a secondary structure of a protein have a slower rate than in corresponding short model peptides.[29,35,36] It has been argued that the Asu ring formation requires specific ranges of dihedral angles that are not energetically favorable in α-helices, β-sheets, and β-turns.[4] This structure-related rate reduction was not observed in this CDR hot spot.

On the contrary, Figure 8b shows that the isomerization rate of D30 on the light-chain CDR1 in the Fab protein is higher than that of the DIDDDM model peptides at pH 5.5 and 6.5. Note that the protein rate considers only the D30 reaction (corresponding to D3 in the DIDDDM peptide), whereas the DIDDDM peptide degradation consists of degradation on all Asp residues; the actual difference in rate between the D30 in protein and D3 in peptide should be even larger. This is an interesting case, different from what has been mostly reported, as stated above. The highly exposed CDR loop that adopts a flexible backbone conformation may give rise to higher probability of solvent–protein proton exchange and favorable phi–psi angles for the amide attacking; however, the rate should still not exceed that in a secondary structure-free peptide; therefore, factors other than solvent exposure and backbone flexibility may account for the higher rate in protein. One such example was reported by Wakankar et al.,[7] showing that the reactive Asp locates within hydrogen-bonding distance with a tyrosine residue. The proton-donating Tyr may accelerate the isomerization reaction. In our case, the crystal structure does not reveal any hydrogen bonding with potential proton donor at pH 5 and above. Besides, the D30 resides in an Asp-rich electronegative patch (data not shown), which should result in suppression of the isomerization rate as argued with the neighboring charge effect. Although the rest of the Asp residues are muted, the D30 isomerized at a surprisingly high rate. One fact that supports the fast isomerization of D30 is the calculated pK_a based on the crystal structure and PROPKA software (Jensen Research Group, Department of Chemistry, University of Copenhagen, Denmark); D30 has a higher pK_a than D31 (4.16 vs. 3.72). Another potential factor is that the backbone may be locked in certain conformation that favors Asu formation on D30. Further studies are required to investigate the structural factors closely to search for the mechanism of higher rate in the protein.

CONCLUSIONS

This study presented the characterization of DD isomerization in both model hexapeptides and antibody fragment CDRs. The isomerization rates were determined for each specific Asp residue in DD-containing peptides. Rate-pH profiles of model peptides and the Fab protein were obtained by stressing samples at various pH values. Compared with the extensively studied DG motif, the DD motif showed great pH dependence in the range of pH 3.6–9. The pH dependence of D3 in YADDFK can be linked to charge on D4. The charge effect of the $n + 1$ residue was confirmed by comparing DD, DN, and DH peptides. The positively charged side chain at the $n + 1$ position resulted in faster isomerization than the neutral side chain, with the negatively charged being the slowest, presumably, primarily by stabilizing or destabilizing the negatively charged tetrahedral intermediate. For the DD peptides, the charge effect seemed to be a mutual impact between the two Asp residues. Protein structural effect was shown by comparing the rate-pH profile of peptide models to that of protein. An interesting case of protein isomerizing faster than peptide, presumably because of contribution from structural factors, was presented. Further studies are required to understand the mechanism. With all of these results, we want to highlight DD as an important hotspot when considering mAb formulations.

ACKNOWLEDGMENTS

The authors thank Kevin Ng for Biomek® robotic setup, Menno van Lookeren Campagne for providing the crystal structure of the Fab, Tom Patapoff for helpful discussion, and Eileen Y. Ivasauskas for editorial assistance.

REFERENCES

1. Manning MC, Chou DK, Murphy BM, Payne RW, Katayama DS. 2010. Stability of protein pharmaceuticals: An update. Pharm Res 27(4):544–575.
2. Bernhard SA, Berger A, Carter JH, Katchalski E, Sela M, Shalitin Y. 1962. Cooperative effects of functional groups in peptides. I. Aspartyl–serine derivatives. J Am Chem Soc 84:2421–2434.
3. Bodanszky M, Natarajan S. 1975. Side reactions in peptide synthesis. II. Formation of succinimide derivatives from aspartyl residues. J Org Chem 40(17):2495–2499.
4. Geiger T, Clarke S. 1987. Deamidation, isomerization, and racemization at asparaginyl and aspartyl residues in peptides. Succinimide-linked reactions that contribute to protein degradation. J Biol Chem 262(2):785–794.
5. Robinson NE, Robinson AB. 2004. Molecular clocks: Deamidation of asparaginyl and glutaminyl residues in peptides and proteins. Cave Junction, Oregon: Althouse Press.
6. Harris RJ, Kabakoff B, Macchi FD, Shen FJ, Kwong M, Andya JD, Shire SJ, Bjork N, Totpal K, Chen AB. 2001. Identification of multiple sources of charge heterogeneity in a recombinant antibody. J Chromatogr B 752(2):233–245.
7. Wakankar AA, Borchardt RT, Eigenbrot C, Shia S, Wang YJ, Shire SJ, Liu JL. 2007. Aspartate isomerization in the complementarity-determining regions of two closely related monoclonal antibodies. Biochemistry 46(6):1534–1544.
8. Tsuda T, Uchiyama M, Sato T, Yoshino H, Tsuchiya Y, Ishikawa S, Ohmae M, Watanabe S, Miyake Y. 1990. Degradation peptides of secretin after storage in acid and neutral aqueous solutions. J Pharm Sci 79(1):53–56.
9. Cacia J, Keck R, Presta LG, Frenz J. 1996. Isomerization of an aspartic acid residue in the complementarity-determining regions of a recombinant antibody to human IgE: Identification and effect on binding affinity. Biochemistry 35(6):1897–1903.
10. Oliyai C, Borchardt RT. 1993. Chemical pathways of peptide degradation. IV. Pathways, kinetics, and mechanism of degradation of an aspartyl residue in a model hexapeptide. Pharm Res 10(1):95–102.
11. Oliyai C, Borchardt RT. 1994. Chemical pathways of peptide degradation. VI. Effect of the primary sequence on the pathways of degradation of aspartyl residues in model hexapeptides. Pharm Res 11(5):751–758.
12. Bongers J, Heimer EP, Lambros T, Pan YC, Campbell RM, Felix AM. 1992. Degradation of aspartic acid and asparagine residues in human growth hormone-releasing factor. Int J Pept Protein Res 39(4):364–374.
13. Johnson BA, Shirokawa JM, Hancock WS, Spellman MW, Basa LJ, Aswad DW. 1989. Formation of isoaspartate at two distinct sites during in vitro aging of human growth hormone. J Biol Chem 264(24):14262–14271.
14. Kirsch LE, Molloy RM, Debono M, Baker P, Farid KZ. 1989. Kinetics of the aspartyl transpeptidation of daptomycin, a novel lipopeptide antibiotic. Pharm Res 6(5):387–393.
15. Radkiewicz JL, Zipse H, Clarke S, Houk KN. 2001. Neighboring side chain effects on asparaginyl and aspartyl degradation: An ab initio study of the relationship between peptide conformation and backbone NH acidity. J Am Chem Soc 123(15):3499–3506.
16. Stephenson RC, Clarke S. 1989. Succinimide formation from aspartyl and asparaginyl peptides as a model for the spontaneous degradation of proteins. J Biol Chem 264(11):6164–6170.
17. Bodanszky M, Kwei JZ. 1978. Side reactions in peptide synthesis. VII. Sequence dependence in the formation of aminosuccinyl derivatives from beta-benzyl-aspartyl peptides. Int J Pept Protein Res 12(2):69–74.
18. Brennan TV, Clarke S. 1995. Effect of adjacent histidine and cysteine residues on the spontaneous degradation of asparaginyl-containing and aspartyl-containing peptides. Int J Pept Protein Res 45(6):547–553.
19. Rehder DS, Chelius D, McAuley A, Dillon TM, Xiao G, Crouse-Zeineddini J, Vardanyan L, Perico N, Mukku V, Brems DN, Matsumura M, Bondarenko PV. 2008. Isomerization of a single aspartyl residue of anti-epidermal growth factor receptor immunoglobulin gamma 2 antibody highlights the role avidity plays in antibody activity. Biochemistry 47(8):2518–2530.
20. Wakankar AA, Borchardt RT. 2006. Formulation considerations for proteins susceptible to asparagine deamidation and aspartate isomerization. J Pharm Sci 95(11):2321–2336.
21. Brennan TV, Clarke S. 1993. Spontaneous degradation of polypeptides at aspartyl and asparaginyl residues—Effects of the solvent dielectric. Protein Sci 2(3):331–338.
22. Xiao G, Bondarenko PV. 2008. Identification and quantification of degradations in the Asp–Asp motifs of a recombinant monoclonal antibody. J Pharm Biomed Anal 47(1):23–30.
23. Zhang J, Yip H, Katta V. 2011. Identification of isomerization and racemization of aspartate in the Asp–Asp motifs of a therapeutic protein. Anal Biochem 410(2):234–243.
24. Ellis KJ, Morrison JF. 1982. Buffers of constant ionic strength for studying pH-dependent processes. Methods Enzymol 87:405–426.
25. Dawson RMC. 1986. Data for biochemical research. Oxford: Clarendon Press.
26. Amano M, Hasegawa J, Kobayashi N, Kishi N, Nakazawa T, Uchiyama S, Fukui K. Specific racemization of heavy-chain cysteine-220 in the hinge region of immunoglobulin gamma 1 as a possible cause of degradation during storage. Anal Chem 83(10):3857–3864.
27. Conrad U, Fahr A, Scriba GKE. 2010. Kinetics of aspartic acid isomerization and enantiomerization in model aspartyl tripeptides under forced conditions. J Pharm Sci 99(10):4162–4173.
28. De Boni S, Oberthur C, Hamburger M, Scriba GK. 2004. Analysis of aspartyl peptide degradation products by high-performance liquid chromatography and high-performance liquid chromatography–mass spectrometry. J Chromatogr A 1022(1–2):95–102.
29. Sadakane Y, Fujii N, Nakagomi K. 2011. Determination of rate constants for β-linkage isomerization of three specific aspartyl residues in recombinant human αA-crystallin protein by reversed-phase HPLC. J Chromatogr B, Anal Technol Biomed Life Sci 879(29):3240–3246.
30. Capasso S, Kirby AJ, Salvadori S, Sica F, Zagari A. 1995. Kinetics and mechanism of the reversible isomerization of aspartic acid residues in tetrapeptides. J Chem Soc, Perkin Trans 2(3):437–442.
31. Capasso S, Mazzarella L, Zagari A. 1991. Deamidation via cyclic imide of asparaginyl peptides: Dependence on salts, buffers and organic solvents. Peptide Res 4(4):234–238.
32. Patel K, Borchardt RT. 1990. Chemical pathways of peptide degradation. II. Kinetics of deamidation of an asparaginyl residue in a model hexapeptide. Pharm Res 7(7):703–711.

33. Li B, Gorman EM, Moore KD, Williams T, Schowen RL, Topp EM, Borchardt RT. 2005. Effects of acidic $N + 1$ residues on asparagine deamidation rates in solution and in the solid state. J Pharm Sci 94(3):666–675.
34. Yu XC, Joe K, Zhang Y, Adriano A, Wang Y, Gazzano-Santoro H, Keck RG, Deperalta G, Ling V. 2011. Accurate determination of succinimide degradation products using high fidelity trypsin digestion peptide map analysis. Anal Chem 83(15):5912–5919.
35. Sinha S, Zhang L, Duan S, Williams TD, Vlasak J, Ionescu R, Topp EM. 2009. Effect of protein structure on deamidation rate in the Fc fragment of an IgG1 monoclonal antibody. Protein Sci 18(8):1573–1584.
36. Xie M, Schowen RL. 1999. Secondary structure and protein deamidation. J Pharm Sci 88(1):8–13.